IQ Imbalance Compensation Scheme in the Presence of Frequency Offset and Dynamic DC Offset for a Direct Conversion Receiver

Mamiko Inamori, *Student Member, IEEE,* Anas M. Bostamam, *Member, IEEE,* Yukitoshi Sanada, *Member, IEEE,* and Hideki Minami, *Member, IEEE*

***Abstract*—A direct conversion architecture reduces the cost and power consumption of a receiver. However, a direct conversion receiver may suffer from direct current (DC) offset, frequency offset, and IQ imbalance. This paper presents an IQ imbalance estimation scheme for orthogonal frequency division multiplexing (OFDM) direct conversion receivers. The proposed IQ imbalance estimation scheme operates in the presence of dynamic DC offset and frequency offset. The proposed scheme calculates IQ imbalance from a simple equation. It employs the knowledge of the preamble symbols of the IEEE 802.11 a/g standards, while it does not require the impulse response of the channel. Numerical results obtained through computer simulation show that the bit error rate (BER) performance for the proposed IQ imbalance estimation scheme has a degradation of about 4dB with a large DC offset, frequency offset, and IQ imbalance.**

***Index Terms*—Direct conversion, OFDM, DC offset, frequency offset, IQ imbalance, training sequence.**

I. Introduction

IEEE 802.11a/g wireless LAN (WLAN) standards are currently used extensively worldwide. In these standards, high-rate data transmission is realized because an orthogonal frequency division multiplexing (OFDM) modulation scheme is used as the 2nd modulation. OFDM achieves high frequency utilization efficiency due to the orthogonality between subcarriers.

At the receiving end, a direct conversion architecture has been implemented, which reduces the cost and power consumption of the receiver. However, OFDM direct conversion receivers may suffer from direct current (DC) offset, frequency offset, and IQ imbalance [1]-[3]. The frequency offset is due to the mismatch between the oscillators in the transmitter and the receiver. The frequency offset at the receiver may deteriorate the orthogonality between the subcarriers and cause intercarrier interference (ICI). The DC offset is caused by the local oscillator (LO) signal. The LO signal can mix with itself down to zero intermediate frequency (IF), resulting in the generation of the DC offset. This is known as self-mixing and is due to the finite isolation that is typical between the LO and the radio frequency (RF) ports of a low-noise amplifier (LNA) or mixers. Moreover, the DC offset is attributed to the mismatch between the mixer components [1], [2]. The IQ imbalance arises mainly from the mismatches between the components between the in-phase (I) and quadrature (Q) paths. Specifically, phase mismatch occurs when the phase difference between the LO signals for the I and Q channels is not exactly 90 degrees [3]. These distortions deteriorate the quality of the demodulated signal. The phase and amplitude mismatches of IQ components are also present in the transmitter [4]. They should be compensated within the received frame since the amount of mismatch depends on the transmitter.

Several joint compensation schemes have been presented [5]-[7]. In [5], the frequency offset and IQ imbalance are estimated using a nonlinear least-squares scheme. This scheme requires the covariance matrix of the received samples. In [6], the IQ imbalance as well as the frequency offset and DC offset are estimated using the maximum likelihood criterion. Although this scheme achieves a performance close to the Cramer-Rao bound, it requires a large amount of computation and channel response. In [7], a frequency offset and IQ imbalance estimation scheme is proposed on the basis of simple calculation. The scheme in [8] carries out frequency offset and IQ imbalance estimation in the time domain. However, these schemes assume the absence of DC offset. The IQ imbalance estimation scheme presented in [9] is conducted in the frequency domain. It requires sufficient time to convert the received signal in the frequency domain by discrete Fourier transform (DFT). However, the length of the preamble signal in the IEEE 802.11a/g standards is quite short. Moreover, the channel estimation needs to be conducted during the period of a long preamble. Therefore, it is necessary to compensate the IQ imbalance immediately after the reception of a short preamble, and the estimation in the frequency domain may not be appropriate [10], [11]. Blind estimation and compensation schemes in the time domain have also been proposed [12]-[14]. Although the amount of computation for each iteration of the adaptive processes is relatively small, these schemes do not assume a dynamic DC offset. If a dynamic DC offset is present, the convergence time may exceed the duration of the short preamble.

The level of DC offset varies due to the gain switching in the LNA. However, none of the above studies take into account the dynamic DC offset, frequency offset, and IQ imbalance at the same time.

In this paper, a novel IQ imbalance estimation scheme is investigated allowing for dynamic DC offset and frequency offset. In the proposed scheme, a differential filter is employed to remove the dynamic DC offset. In previous research, it has been shown that the differential filter effectively estimates

Manuscript received February 2, 2008; revised June 30, 2008 and October 29, 2008; accepted December 12, 2008. The associate editor coordinating the review of this letter and approving it for publication was M. Morelli.

M. Inamori, A. M. Bostamam, and Y. Sanada are with the Dept. of Electronics and Electrical Engineering, Keio University, 3-14-1 Hiyoshi, Kohoku, Yokohama, 223-8522 Japan (e-mail: {mamiko, anas}@snd.elec.keio.ac.jp, sanada@elec.keio.ac.jp).

H. Minami is with Sony Corporation, Atsugi, 243-0014 Japan (e-mail: minami@sabip.semicon.sony.co.jp).

Digital Object Identifier 10.1109/TWC.2009.080139

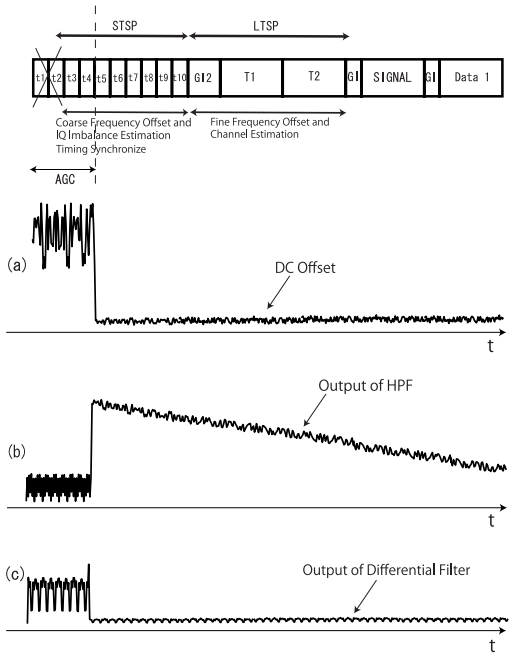

Fig. 1. DC offset and the output of differential filter.

frequency offset in the presence of dynamic DC offset [15]-[17]. In the proposed scheme, from the output of the differential filter, the IQ imbalance as well as the frequency offset is estimated from a simple equation. The proposed scheme employs the knowledge of the preamble symbols of the IEEE 802.11a/g standards, while it does not require the impulse response of the channel. Therefore, this scheme is suitable for low-cost and low-power-consumption receivers.

This paper is organized as follows. Section II gives the system model and the IQ imbalance model. In Section III, the frequency offset estimation using the differential filter is explained. Section IV describes the proposed IQ imbalance estimation. In Section V numerical results obtained through computer simulation are presented. Section VI gives our conclusions.

II. System Model

A. Preamble Model

Figure 1 shows the IEEE 802.11a/g burst structure of the preamble signal [10], [11]. In the 802.11a/g preamble, short training sequence preamble (STSP) symbols are used for coarse frequency offset estimation and IQ imbalance estimation. Long training sequence preamble (LTSP) symbols are used for fine frequency offset estimation and channel estimation.

The STSP symbols consist of 12 subcarrier signals, which are repeated with a period of $0.8\mu s$ $(= T_{FFT}/4 = 3.2/4)$, where T_{FFT} is the fast Fourier transform (FFT) and inverse FFT (IFFT) period. On the other hand, the LTSP symbols consist of 52 subcarrier signals, which have two periods of $3.2\mu s$ $(= T_{FFT})$. During the period of the LTSP, the OFDM training symbols for channel estimation are transmitted [10], [11]. Therefore, frequency offset needs to be estimated appropriately during the period of coarse estimation.

B. Subcarrier Allocation

In IEEE 802.11a/g, the subcarrier at zero frequency is not used. In practice, this is to avoid interference from the DC offset. Although the subcarriers do not interfere with each other, if frequency offset exists, the orthogonality between the subcarriers and the DC offset is deteriorated. However, as the zero-frequency subcarrier is not used, if the synthesizers are ideally synchronized, the DC offset does not interfere with the OFDM subcarriers. A high-pass filter (HPF) can be used to eliminate the static DC offset without removing the received signal.

C. Automatic Gain Control and Differential Filter

To maintain the received signal amplitude at a suitable fixed level, automatic gain control (AGC) is used. In a WLAN receiver, the AGC controls the receiver gain in the middle of the STSP. In the 802.11a/g standards, gain control of more than 50dB is required [18]. The assumed RF architecture in this paper is shown in Fig. 2. As shown in the figure, gain control is applied in both the LNA and the variable gain amplifiers (VGAs). Here, an LNA with two gain modes is assumed [19]-[21]. This type of LNA has been discussed in [19] and [22]. The VGAs at baseband compensate the rest of the required gain.

In the direct conversion receiver, the DC offset may be eliminated by HPFs, as shown in Fig. 2 [1], [19]. However, as the gain of the LNA changes, the DC offset level varies [23]. Figures 1 (a), (b), and (c) show the received signal (absolute value) of the training sequence preamble when the gain of the LNA is changed. At the beginning of the STSP, the gain of the LNA is set to the maximum because the power of the received signal is unknown to the receiver. If the power of the received signal is sufficiently large, the LNA is switched to the low-gain mode between t_4 and t_5. The DC offset level then decreases rapidly and the fluctuating DC offset level is input into the HPF. Here, the fluctuation of the DC offset level is modeled as a two-step function as shown in Fig. 1 (a) [23]. The transient response of the HPF due to the fluctuation of the DC offset level appears at the output of the HPF as shown in Fig. 1 (b). The component deteriorates the accuracy of frequency offset estimation and IQ imbalance estimation. In the proposed scheme, the transient response is removed using the differential filter. The cutoff frequency of the HPF is set to relatively low so as not to eliminate the data subcarriers adjacent to the DC subcarrier in the data period. Since the cutoff frequency of the HPF is low, the transient response decreases gradually. Thus, the differential filter can suppress the effect of the residual DC offset as shown in Fig. 1 (c).

D. IQ Imbalance

The direct conversion architecture is suitable for mobile terminals since it does not require costly IF filters and allows for single-chip integration. However, because of the absence of a digital IF, IQ demodulation is not handled in the digital domain, but in the analog domain. Therefore, the direct conversion receiver introduces the so-called IQ imbalance in the mixers, as shown in Fig. 2. In the figure, the phase mismatch and gain mismatch are represented as θ and β,

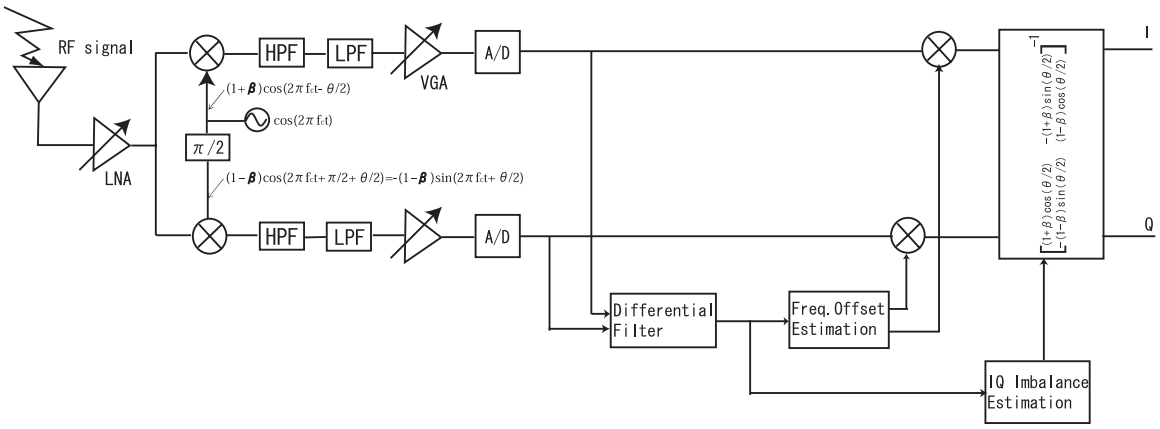

Fig. 2. Receiver architecture.

respectively. This IQ imbalance is mainly attributed to the mismatched components along the I and Q paths. Specifically, phase mismatch occurs when the phase difference between the local oscillator's signals for the I and Q channels is not exactly 90 degrees. Gain imbalance refers to the gain mismatch in the path of the I and Q signals [3].

Assuming that the kth digitized sample of the OFDM preamble in the time domain is $s(k)$, the received signal with frequency offset, $r(k)$, is expressed as

$$r(k) = s(k)\exp(j\frac{2\pi\alpha}{N}k) + \omega(k), \tag{1}$$

where N is the number of samples used for DFT, α is the frequency offset normalized by subcarrier separation, and $\omega(k)$ is the kth AWGN sample with zero mean and variance N_0. In this paper, because of the symmetry of the upper and lower paths, the I-phase local signal, L_I, and the Q-phase local signal, L_Q, are assumed to be as follows:

$$\begin{array}{ll} \text{I component} & L_I = (1+\beta)\cos(2\pi f_c t - \theta/2), \\ \text{Q component} & L_Q = -(1-\beta)\sin(2\pi f_c t + \theta/2), \end{array}$$

where f_c is the carrier frequency. These local signals are multiplied by the received signal, and by applying the LPF, the baseband signals, $\hat{r}_I(k)$ and $\hat{r}_Q(k)$, with IQ imbalance are obtained. The kth digitized signal with a sampling interval of T_s is given by

$$\hat{r}(k) = \hat{r}_I(k) + j\hat{r}_Q(k), \tag{2}$$

where

$$\hat{r}_I(k) = (1+\beta)\{r_I(k)\cos(\frac{\theta}{2}) - r_Q(k)\sin(\frac{\theta}{2})\}, \tag{3}$$

$$\hat{r}_Q(k) = (1-\beta)\{r_Q(k)\cos(\frac{\theta}{2}) - r_I(k)\sin(\frac{\theta}{2})\}, \tag{4}$$

where $r_I(k)$ and $r_Q(k)$ are the I component and Q component of $r(k)$, respectively. Hence, the complex baseband signal $\hat{r}(k)$ is

$$\begin{aligned} \hat{r}(k) &= \hat{r}_I(k) + j\hat{r}_Q(k) \\ &= \{\cos(\frac{\theta}{2}) + j\beta\sin(\frac{\theta}{2})\}\{r_I(k) + jr_Q(k)\} \\ &\quad + \{\beta\cos(\frac{\theta}{2}) - j\sin(\frac{\theta}{2})\}\{r_I(k) - jr_Q(k)\} \\ &= \{\cos(\frac{\theta}{2}) + j\beta\sin(\frac{\theta}{2})\}r(k) \\ &\quad + \{\beta\cos(\frac{\theta}{2}) - j\sin(\frac{\theta}{2})\}r^*(k), \end{aligned} \tag{5}$$

where the * denotes the complex conjugate.

III. Frequency Offset Estimation

A. Frequency Offset, DC Offset, and IQ Imbalance Model

In order to clarify the signal model with frequency offset, DC offset, and IQ imbalance, the following explanation omits the noise term, $\omega(k)$, in Eq. (1) for simplicity. From Eq. (5), the received signal with the IQ imbalance is given as

$$\hat{r}(k) = \phi r(k) + \psi^* r^*(k) + \delta(k), \tag{6}$$

where

$$\phi = \cos(\frac{\theta}{2}) + j\beta\sin(\frac{\theta}{2}), \tag{7}$$

$$\psi = \beta\cos(\frac{\theta}{2}) + j\sin(\frac{\theta}{2}), \tag{8}$$

and $\delta(k)$ is the DC offset that occurs at the mixer.

The frequency offset is estimated in the presence of the dynamic DC offset and the IQ imbalance. After coarse estimation, the LTSP symbols are used for channel estimation for each subcarrier.

B. Frequency Offset Estimation Using Differential Filter

In this frequency offset estimation scheme, the received signal with IQ imbalance is substituted into the differential filter used to eliminate the residual DC offset that passes

through the HPF. The kth output $\hat{d}_{SP}(k)$ after the differential filter is

$$\begin{aligned}\hat{d}_{SP}(k) &= \hat{r}_{SP}(k) - \hat{r}_{SP}(k-1) \\ &= \phi\{r_{SP}(k) - r_{SP}(k-1)\} \\ &\quad + \psi^*\{r^*_{SP}(k) - r^*_{SP}(k-1)\} \\ &\quad + \Delta\delta(k, k-1),\ k \geq 1, \end{aligned} \tag{9}$$

where

$$\hat{r}_{SP}(k) = \phi r_{SP}(k) + \psi^* r^*_{SP}(k), \tag{10}$$

$r_{SP}(k)$ is the kth signal with the frequency offset in the STSP period, and $\Delta\delta(k, k-1)$ is the difference between the kth and $(k-1)$th residual DC offsets. In the STSP, a short preamble with a period of $N/4$ samples is repeated 10 times. From Eq. (9), the autocorrelation value for frequency offset estimation with the DC offset and the IQ imbalance is given by

$$\begin{aligned}&\hat{d}^*_{SP}(k)\hat{d}_{SP}(k+\frac{N}{4}) \\ =\ & |\phi|^2 |r_{SP}(k+\tfrac{N}{4}) - r_{SP}(k+\tfrac{N}{4}-1)|^2 \exp(j\frac{2\pi\alpha}{4}) \quad (11a) \\ &+\phi^*\psi^*(r_{SP}(k+\tfrac{N}{4}) - r_{SP}(k+\tfrac{N}{4}-1))^2 \exp(-j\frac{2\pi\alpha}{4}) \quad (11b) \\ &+\phi\psi(r_{SP}(k+\tfrac{N}{4}) - r_{SP}(k+\tfrac{N}{4}-1))^2 \exp(j\frac{2\pi\alpha}{4}) \quad (11c) \\ &+|\psi|^2 |r_{SP}(k+\tfrac{N}{4}) - r_{SP}(k+\tfrac{N}{4}-1)|^2 \exp(-j\frac{2\pi\alpha}{4}) \quad (11d) \\ &+O(\Delta\delta(k+\tfrac{N}{4}, k+\tfrac{N}{4}-1), \Delta\delta(k, k-1)). \quad (11e)\end{aligned}$$

Here, $O(\Delta\delta(k+\frac{N}{4}, k+\frac{N}{4}-1), \Delta\delta(k, k-1))$ is the product of $\Delta\delta(k+\frac{N}{4}, k+\frac{N}{4}-1)$ and $\Delta\delta(k, k-1)^*$, N is the number of samples, and α is the normalized frequency offset in one OFDM symbol period. By averaging over 10 STSP symbols, the normalized frequency offset α is estimated from the first term (11a). The additional mean square error (MSE) in frequency offset estimation due to the IQ imbalance is caused by the terms given in (11b), (11c), and (11d). However, it is less than 10^{-3} of the square of the frequency offset [17]. Thus, the IQ imbalance is neglected at this stage for estimation of the frequency offset.

IV. IQ Imbalance Estimation

A. IQ Imbalance Estimation

The IQ imbalance is also estimated from the outputs of the differential filter. From Eq. (9), the 3 preamble symbols repeated in $N/4$ samples in the STSP can be expressed as

$$\begin{aligned}\hat{d}_{SP}(k-\frac{N}{4}) &= \hat{r}_{SP}(k-\frac{N}{4}) - \hat{r}_{SP}(k-\frac{N}{4}-1) \\ &= \phi\{r_{SP}(k) - r_{SP}(k-1)\}\exp(-j\frac{2\pi\alpha}{4}) \\ &\quad + \psi^*\{r^*_{SP}(k) - r^*_{SP}(k-1)\}\exp(j\frac{2\pi\alpha}{4}) \\ &= \phi d_{SP}(k)\gamma^{-1} + \psi^* d^*{}_{SP}(k)\gamma, \end{aligned} \tag{12}$$

$$\begin{aligned}\hat{d}_{SP}(k) &= \hat{r}_{SP}(k) - \hat{r}_{SP}(k-1) \\ &= \phi\{r_{SP}(k) - r_{SP}(k-1)\} \\ &\quad + \psi^*\{r^*_{SP}(k) - r^*_{SP}(k-1)\} \\ &= \phi d_{SP}(k) + \psi^* d^*{}_{SP}(k), \end{aligned} \tag{13}$$

$$\begin{aligned}\hat{d}_{SP}(k+\frac{N}{4}) &= \hat{r}_{SP}(k+\frac{N}{4}) - \hat{r}_{SP}(k+\frac{N}{4}-1) \\ &= \phi\{r_{SP}(k+\tfrac{N}{4}) - r_{SP}(k+\tfrac{N}{4}-1)\} \\ &\quad + \psi^*\{r^*_{SP}(k+\tfrac{N}{4}) - r^*_{SP}(k+\tfrac{N}{4}-1)\} \\ &= \phi\{r_{SP}(k) - r_{SP}(k-1)\}\exp(j\frac{2\pi\alpha}{4}) \\ &\quad + \psi^*\{r^*_{SP}(k) - r^*_{SP}(k-1)\}\exp(-j\frac{2\pi\alpha}{4}) \\ &= \phi d_{SP}(k)\gamma + \psi^* d^*{}_{SP}(k)\gamma^{-1}. \end{aligned} \tag{14}$$

Here,

$$d_{SP}(k) = r_{SP}(k) - r_{SP}(k-1), \tag{15}$$

$$\gamma = \exp(j\frac{2\pi\alpha}{4}). \tag{16}$$

Solving Eqs. (12), (13), and (14) as simultaneous equations, the following equation is derived.

$$\frac{\hat{d}_{SP}(k-\frac{N}{4}) - \hat{d}_{SP}(k)\gamma^{-1}}{(\hat{d}_{SP}(k)\gamma^{-1} - \hat{d}_{SP}(k+\frac{N}{4}))^*} = \frac{\psi^*}{\phi^*} = \varepsilon. \tag{17}$$

Here, with the assumption of small θ, ϕ and ψ are approximated as

$$\phi = \cos(\frac{\theta}{2}) + j\beta\sin(\frac{\theta}{2}) \approx 1 + j\beta\frac{\theta}{2}, \tag{18}$$

$$\psi = \beta\cos(\frac{\theta}{2}) + j\sin(\frac{\theta}{2}) \approx \beta + j\frac{\theta}{2}, \tag{19}$$

using the first-order approximation of the Taylor expansion. Thus, Eq. (17) becomes

$$\frac{\beta - j\frac{\theta}{2}}{1 - j\beta\frac{\theta}{2}} \approx \varepsilon_I + j\varepsilon_Q. \tag{20}$$

β and θ can then be calculated as follows.

$$\beta \approx \frac{2\varepsilon_I}{2 - \varepsilon_Q\theta}, \tag{21}$$

$$\theta \approx \frac{-(\varepsilon_I^2 + \varepsilon_Q^2 - 1) - \sqrt{(\varepsilon_I^2 + \varepsilon_Q^2 - 1)^2 + 4\varepsilon_Q^2}}{\varepsilon_Q}. \tag{22}$$

To obtain ε in Eq. (17), α in Eq. (16) is substituted with the value estimated in Section III.

In terms of complexity, the estimation of ε requires the following number of calculations;

$$C_\varepsilon = N_{sp} \times [2{\cdot}C_{add} + 1{\cdot}C_{mult}] + 1{\cdot}C_{div}, \tag{23}$$

where C_{add}, C_{mult}, and C_{div} are the numbers of complex additions, multiplications, and divisions, respectively, and N_{sp} represents the number of samples in the STSP. The complexity is almost equivalent to the conventional scheme in [8].

Note that, similar to [8], the proposed scheme works well if α is more than 0.1. This can be understood by taking the noise term into consideration in Eq. (17). If the noise is included, the left side of Eq. (17) turns to Eq. (24) at the top of this page.

$$\frac{\psi^*\{s^*_{SP}(k)\exp(-j\frac{2\pi\alpha}{N}k) - s^*_{SP}(k-1)\exp(-j\frac{2\pi\alpha}{N}(k-1))\}(\gamma-\gamma^{-1}) + O(\phi,\psi,\gamma^{-1},\omega(k-\frac{N}{4}-1),\omega(k-\frac{N}{4}),\omega(k-1),\omega(k))}{\phi^*\{s^*_{SP}(k)\exp(-j\frac{2\pi\alpha}{N}k) - s^*_{SP}(k-1)\exp(-j\frac{2\pi\alpha}{N}(k-1))\}(\gamma-\gamma^{-1}) + O(\phi,\psi,\gamma,\omega(k-1),\omega(k),\omega(k+\frac{N}{4}-1),\omega(k+\frac{N}{4}))}. \quad (24)$$

Here, $O(\phi,\psi,\gamma^{-1},\omega(k-\frac{N}{4}-1),\omega(k-\frac{N}{4}),\omega(k-1),\omega(k))$ is the product of ϕ, ψ, γ^{-1}, $\omega(k-\frac{N}{4}-1)$, $\omega(k-\frac{N}{4})$, $\omega(k-1)$, $\omega(k)$. $O(\phi,\psi,\gamma,\omega(k-1),\omega(k),\omega(k+\frac{N}{4}-1),\omega(k+\frac{N}{4}))$ is also the product of ϕ, ψ, γ, $\omega(k-1)$, $\omega(k)$, $\omega(k+\frac{N}{4}-1)$, $\omega(k+\frac{N}{4})$. If the frequency offset α is small, the term $(\gamma-\gamma^{-1})$ approaches to 0. The left side of Eq. (17) is then approximated as

$$\frac{\hat{d}_{SP}(k-\frac{N}{4}) - \hat{d}_{SP}(k)\gamma^{-1}}{(\hat{d}_{SP}(k)\gamma^{-1} - \hat{d}_{SP}(k+\frac{N}{4}))^*} \approx \frac{O(\phi,\psi,\gamma,\omega(k-\frac{N}{4}-1),\omega(k-\frac{N}{4}),\omega(k-1),\omega(k))}{O(\phi,\psi,\gamma,\omega(k-1),\omega(k),\omega(k+\frac{N}{4}-1),\omega(k+\frac{N}{4}))}. \quad (25)$$

Thus, the estimation of IQ imbalance becomes inaccurate. In this case, the time difference among the outputs of the differential filter in Eqs. (12), (13), and (14) should be set to longer than $N/4$. The effective frequency offset then increases although the number of samples required to calculate Eq. (17) decreases.

B. IQ Imbalance Compensation

In the LTSP and the following data period, IQ imbalance is compensated on the basis of the phase mismatch and gain mismatch estimated in the STSP. By consolidating Eqs. (7) and (8) into a system of equations, we arrive at

$$\begin{bmatrix} \hat{r}_{d_I} \\ \hat{r}_{d_Q} \end{bmatrix} = \begin{bmatrix} (1+\beta)\cos(\frac{\theta}{2}) & -(1+\beta)\sin(\frac{\theta}{2}) \\ -(1-\beta)\sin(\frac{\theta}{2}) & (1-\beta)\cos(\frac{\theta}{2}) \end{bmatrix} \begin{bmatrix} r_{d_I} \\ r_{d_Q} \end{bmatrix} = \mathbf{\Omega} \begin{bmatrix} r_{d_I} \\ r_{d_Q} \end{bmatrix}, \quad (26)$$

where $\hat{r}_{d_I}$, $\hat{r}_{d_Q}$, r_{d_I}, and r_{d_Q} are the I and Q components of the received signal with and without IQ imbalance, respectively. The IQ imbalance is compensated using $\mathbf{\Omega}^{-1}$.

V. Simulation Results

A. Simulation Conditions

The MSE of the IQ imbalance estimation is evaluated through computer simulation. The number of trials is 10,000 times. Information bits are modulated with QPSK in the preamble period and 64QAM in the data period on each subcarrier. The number of DFT/IDFT points is set to 64, while 48 subcarriers are used for the data subcarriers and 4 subcarriers are used for the pilot subcarriers, which follows the IEEE 802.11a/g standards. As a channel model, AWGN channel is assumed. A 1st-order Butterworth filter is employed as the HPF. The cutoff frequency of the HPF is set to 10[kHz]. The normalized frequency offset, α, is 0.3. The gain mismatch is set from 0.01 to 0.05 and the phase mismatch is set from 0 to 5[degree] [8].

The gain of the LNA can be selected between 35 and 15[dB] [24]. The isolation between the LO output and the LNA input is assumed to be -60[dB]. Therefore, if the power of the LO signal is set to 0[dBm], the DC offset level is -25/-45[dBm].

On the other hand, the received signal power is set to -53[dBm], which is equivalent to -70[dBm] on each subcarrier in the LTSP. In this case, the DC offset is 10[dB] larger than the signal power on each subcarrier.

1) Normalized MSE Performance of Phase Mismatch Estimation vs. Phase Mismatch: Figure 3 shows the normalized MSE performance of phase mismatch estimation. In this figure, 'Conventional' refers to the IQ imbalance estimation scheme in the time domain presented in [8]. The gain mismatch β is set to 0.05 and the normalized frequency offset α is set to 0.3. In Fig. 3, the proposed scheme has better estimation performance.The reason for this is that the conventional scheme suffers from the residual DC offset. In this figure, the MSE improves as the phase mismatch increases. This is because the MSE is normalized by the mismatch θ. Furthermore, the normalized MSE performance improves as E_b/N_0 increases from 20 to 25[dB]. The normalized MSE of the phase mismatch θ fluctuates when E_b/N_0=20[dB]. This is because Eq. (22) has ε_Q in the denominator. If the estimated value of ε_Q approaches 0 due to noise, the MSE of the phase mismatch, θ, increases. This case rarely happens and does not change the average BER.

2) Normalized MSE Performance of Phase Mismatch Estimation vs. Frequency Offset: Figure 4 shows the normalized MSE performance of phase mismatch estimation with dynamic DC offset and frequency offset when the frequency offset is varied. The gain mismatch β is set to 0.05 and the phase mismatch θ is set to 5[degree]. E_b/N_0 in the LTSP is set to {20, 25, or 30}[dB].

It is clear from Fig. 4 that the normalized MSE performance increases as the frequency offset reduces. This is because the term $(\gamma-\gamma^{-1})$ in Eq. (24) approaches to 0 as mentioned in Section IV-A.

3) Normalized MSE Performance of Gain Mismatch Estimation: Figure 5 shows the normalized MSE performance of the gain mismatch estimation with dynamic DC offset and frequency offset when the gain mismatch value is varied. The phase mismatch θ is set to 5[degree] and the normalized frequency offset α is set to 0.3. E_b/N_0 in the LTSP is set to {20, 25, or 30}[dB].

It can be seen from Fig. 5 that the normalized MSE performance improves as the gain mismatch increases. This is because the MSE is normalized by the gain mismatch β. As E_b/N_0 increases to 10[dB], the normalized MSE is reduced by a factor of about 10.

4) BER Performance: The BER performance versus E_b/N_0 in the AWGN channel is shown in Fig. 6. The simulation conditions are the same as those with the static DC offset. From Fig. 6, it can be concluded that the performance degradation due to the proposed scheme is about 4[dB]. This plot is simulated using 1st order interpolation for phase compensation using pilot subcarriers. 125 OFDM symbols

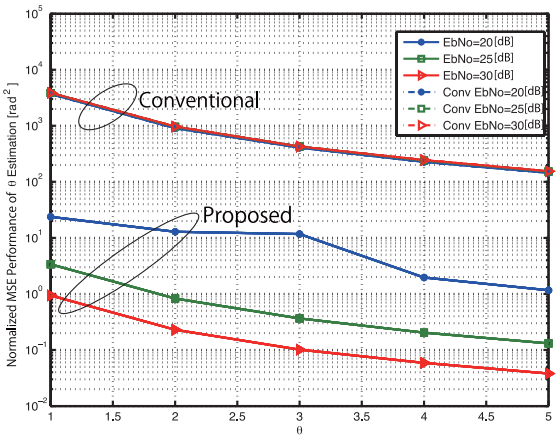

Fig. 3. Normalized MSE performance of phase mismatch estimation vs. phase mismatch (β=0.05, normalized freq. offset = 0.3).

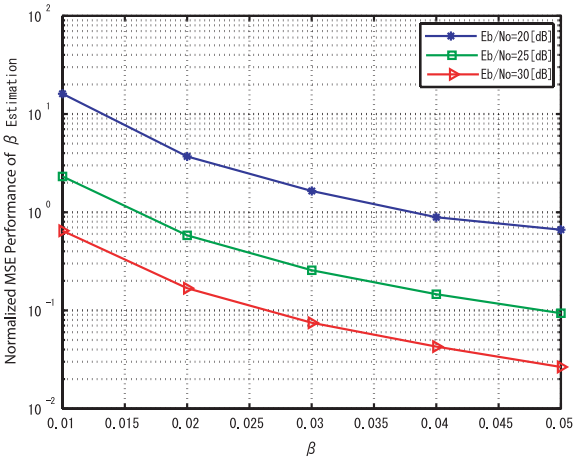

Fig. 5. Normalized MSE performance of gain mismatch estimation (θ= 5[degree], normalized freq. offset=0.3).

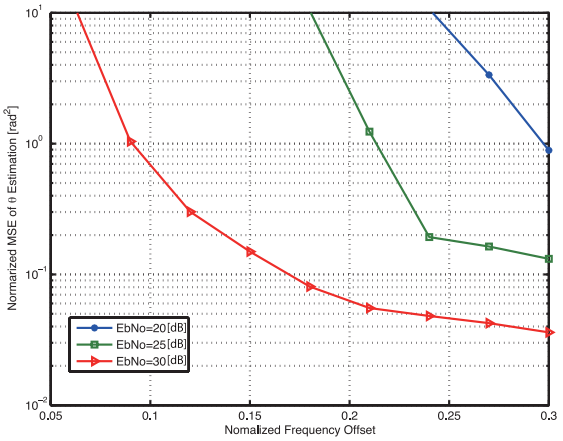

Fig. 4. Normalized MSE performance of phase mismatch estimation vs. frequency offset (β=0.05, θ= 5[degree]).

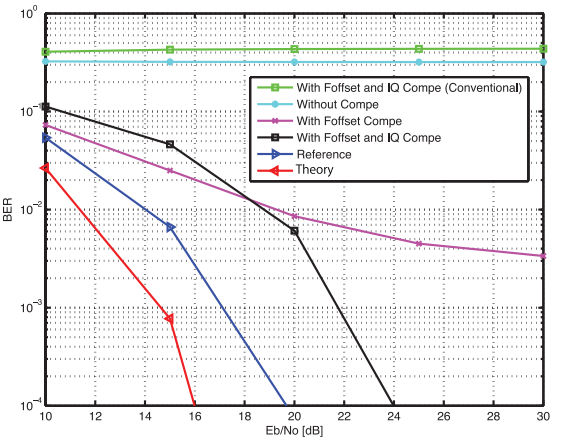

Fig. 6. BER performance with 1st interpolation (normalized freq. offset=0.3, β=0.05, θ=5[degree]).

are transmitted for each packet and 64QAM is assumed. The number of DFT/IDFT points is set to 64. The OFDM receiver is considered with normalized frequency offset $\alpha = 0.3$, gain imbalance $\beta = 0.05$, and phase mismatch $\theta = 5$[degree].

'With Foffset and IQ Compe (Conventional)' refers to the case with frequency offset compensation and IQ imbalance compensation presented in [8]. 'Without Compe' represents the simulation in the case of no frequency offset compensation or IQ imbalance compensation, 'With Foffset Compe' refers to frequency offset compensation, and 'With Foffset and IQ Compe' refers to the case of frequency offset compensation and IQ imbalance compensation. In addition, 'Reference' represents the simulation when phase compensation by pilot subcarriers is carried out under frequency offset and IQ imbalance. In each OFDM symbol, following the IEEE 802.11 a/g standards, 4 pilot subcarriers are inserted. 'Theory' is the theoretical BER curve for 64QAM.

As shown in this figure, the proposed scheme exhibits superior estimation performance since the conventional scheme suffers from the residual DC offset. Moreover, neither frequency offset compensation nor IQ imbalance compensation degrades the performance significantly. Comparing the proposed scheme with theoretical results, there is difference of 8[dB], in which 4[dB] of the difference is due to nonideal channel equalization by the pilot subcarriers. Thus, the BER using the proposed IQ imbalance estimation scheme exhibits about 4[dB] degradation with large DC offset, frequency offset, and IQ imbalance. However, our proposed scheme has less complexity than existing algorithms.

VI. Conclusion

The direct conversion receiver has disadvantages such as DC offset, frequency offset, and IQ imbalance. In this paper, a low-complexity IQ imbalance estimation scheme allowing for dynamic DC offset and frequency offset has been proposed. The IQ imbalance is calculated using a simple equation without requiring the impulse response of the channel. Therefore, the proposed scheme is suitable for low-cost and low-power-consumption terminals. Computer simulations show that the BER performance using the proposed IQ imbalance estimation

scheme is satisfactory when E_b/N_0 is more than 20[dB], in which 64QAM is used for the 1st modulation. The system exhibits a degradation of about 4[dB] with a large dynamic DC offset, a frequency offset, and an IQ imbalance. In future studies we plan to focus on enhancing the estimation accuracy of frequency offset and IQ imbalance recursively over multiple frames.

REFERENCES

[1] W. Namgoong and T. H. Meng, "Direct-conversion RF receiver design," *IEEE Trans. Commun.*, vol. 49, no. 3, pp. 518-529, Mar. 2001.

[2] R. Svitek and S. Raman, "DC offsets in direct-conversion receivers: characterization and implications," *IEEE Microwave Mag.*, vol. 6, no. 3, pp. 76-86, Sept. 2005.

[3] T. Yuba and Y. Sanada, "Decision directed scheme for IQ imbalance compensation on OFCDM direct conversion receiver," *IEICE Trans. Commun.*, vol. E89-E, no. 1, pp. 184-190, Jan. 2006.

[4] D. S. Hilborn, S. P. Stapleton, and H. K. Cavers, "An adaptive direct conversion transmitter," *IEEE Trans. Veh. Technol.*, vol. 43, no. 2, pp. 223-233, May 1994.

[5] G. Xing, M. Shen, and H. Liu, "Frequency offset and I/Q imbalance compensation for direct conversion receivers," *IEEE Trans. Commun.*, vol. 4, pp. 673-680, Mar. 2005.

[6] G. T. Gil, I. H. Sohn, Y. H. Lee, Y. I. Song, and J. K. Park, "Joint ML estimation of carrier frequency, channel, I/Q mismatch, and DC offset in communications receivers," *IEEE Trans. Veh. Technol.*, vol. 54, no. 1, pp. 338-349, Jan. 2005.

[7] S. D. Rore, E. L. Estraviz, F. Horlin, and L. V. Perre, "Joint estimation of carrier frequency offset and IQ imbalance for 4G mobile wireless systems," in *Proc. ICC'06*, vol. 5, pp. 2066-2071, June 2006.

[8] J. Tubbax, A. Fort, L. V. Perre, S. Donnay, M. Moonen, and H. D. Man, "Joint compensation of IQ imbalance and frequency offset in OFDM systems," in *Proc. GLOBECOM'03*, vol. 3, pp. 2365-2369, May 2003.

[9] M. Windisch and G. Fettweis, "On the performance of standard-independent I/Q imbalance compensation in OFDM direct-conversion receivers," in *Proc. 13th European Signal Processing Conf. (EUSIPCO)*, Sept. 2005.

[10] IEEE.802.11a-Part 11, Wireless LAN Medium Access Control (MAC) and Physical Layer (PHY) Specifications; Highspeed Physical Layer in the 5GHz Band.

[11] IEEE.802.11g-Part 11, Wireless LAN Medium Access Control (MAC) and Physical Layer (PHY) Specifications; Highspeed Physical Layer in the 2.4GHz Band.

[12] A. C. Douglas and S. Haykin, "On the relationship between blind deconvolution and blind source separation," in *Proc. ACSSC'97*, vol. 2, pp. 1591-1595, Nov. 1997.

[13] M. Valkama, M. Renfors, and V. Koivunen, "Advanced methods for I/Q imbalance compensation in communication receivers," *IEEE Trans. Signal Processing*, vol. 49, no. 10, pp. 2335-2344, Oct. 2001.

[14] P. Rykaczewski, J. Brakensiek, and F. Jondral, "Decision directed methods of I/Q imbalance compensation in OFDM systems," in *Proc. VTC 2004 Fall*, vol. 1, pp. 484-487, Sept. 2004.

[15] M. Inamori, A. M. Bostamam, Y. Sanada, and H. Minami, "Frequency offset compensation scheme under DC offset for OFDM direct conversion receivers," in *Proc. 9th International Sym. Wireless Personal Multimedia Commun.*, pp. 378-382, San Diego, CA, Sept. 2006.

[16] M. Inamori, A. M. Bostamam, Y. Sanada, and H. Minami, "Frequency offset estimation scheme in the presence of time-varying DC offset for OFDM direct conversion receivers," *IEICE Trans. Commun.*, vol. E90-B, no. 10, pp. 2884-2890, Oct. 2007.

[17] M. Inamori, A. M. Bostamam, Y. Sanada, and H. Minami, "Frequency offset estimation scheme in the presence of time-varying DC offset and IQ imbalance for OFDM direct conversion receivers," in *Proc. 18th Annual International Sym. Personal Indoor Mobile Radio Commun.*, pp. 1-5, Athens, Greece, Sept. 2007.

[18] T. Fujisawa, J. Hasegawa, K. Tsuchie, T. Shiozawa, T. Fujita, T. Saito, and Y. Unekawa, "A single-chip 802.11a MAC/PHY with a 32-b RISC processor," *IEEE J. Solid-State Circuits*, vol. 38, no. 11, pp. 2001-2009, Nov. 2003.

[19] H. Yoshida, T. Kato, T. Toyoda, I. Seto, R. Fujimoto, T. Kimura, O. Watanabe, T. Arai, T. Itakura, and H. Tsurumi, "Fully differential direct conversion receiver for W-CDMA using an active harmonic mixer," in *Proc. IEEE Radio Frequency Integrated Circuit Sym.*, pp. 395-398, June 2003.

[20] J. Olsson, "WLAN/WCDMA dual-mode receiver architecture design trade-offs," in *Proc. IEEE 6th CAS Sym.*, vol. 2, pp. 725-728, May-June 2004.

[21] M. Faulkner, "DC offset and IM2 removal in direct conversion," *IEE Proc. Commun.*, vol. 149, pp. 179-184, June 2002.

[22] R. G. Meyer, W. D. Mack, and J. Hageraats, "A 2.5GHz BiCMOS transceiver for wireless LAN," in *Proc. ISSCC'97*, pp. 310-311, Feb. 1997.

[23] S. Otaka, T. Yamaji, R. Fujimoto, and H. Tanimoto, "A low offset 1.9-GHz direct conversion receiver IC with spurious free dynamic range of over 67 dB," *IEICE Trans. Fundamentals*, vol. E84-A, no. 2, pp. 513-519, Feb. 2001.

[24] T. Liu and E. Westerwick, "5 GHz CMOS radio transceiver front-end chipset," in *Proc. ISSCC Tech. Dig.*, pp. 320-321, Feb. 2000.